Control allocation based fault-tolerant control design for spacecraft attitude tracking

Qiang Shen, Danwei Wang, Senqiang Zhu, and Eng Kee Poh

Abstract— **This paper presents a fault-tolerant control allocation scheme for overactuated spacecraft attitude tracking systems subject to actuator faults. Taking the effect of fault detection and diagnosis (FDD) uncertainties into account, a performance/robustness trade-off control allocation (PRTCA) strategy is proposed to redistribute the virtual control signals to the remaining actuators without reconfiguring the controller. The proposed PRTCA scheme achieves robustness with respect to the imprecise in fault estimation, and is less conservative than the robust control allocation. To illustrate the performance of the proposed PRTCA strategy, numerical simulations are carried out for a rigid spacecraft in the presence of reaction wheel faults.**

I. Introduction

In complex systems like spacecraft, aircraft, and chemical plants, it is increasingly important to ensure their reliability. To enhance the system reliability and safety, the control system has to be capable of tolerating potential faults automatically while maintaining desirable system performance and stability properties. This has motivated a significant amount of research on fault-tolerant control (FTC) strategies [1]–[3]. For spacecraft attitude control systems, actuators play an important role in generating control efforts commanded from the controller to achieve specific mission objectives. However, when a fault occurs in the actuator, the influence of the controller on the spacecraft might be interrupted or modified. As a result, if the controller is designed without any fault tolerance capability, an abrupt occurrence of an actuator fault could significantly degrade mission performance or even lead to totally loss of the spacecraft. Therefore, to enhance the spacecraft reliability and safety, actuator fault tolerance capability need to be addressed in attitude control design.

In order to handle actuator faults, many methods have been proposed to design a fault-tolerant attitude controller for spacecraft in the literature. Depending on how redundancies are utilized, current methods can be classified into two categories: passive and active strategies [5]. In a passive fault-tolerant attitude control system, all potential actuator faults are considered together with the normal system operating conditions at the design stage, and a single fixed fault-tolerant attitude controller on the basis of robust control theory is synthesized so that the attitude control system is able to achieve its given objectives throughout the healthy situation and the faulty situation. In [6], an indirect robust adaptive FTC strategy was proposed to handle actuator failures for attitude tracking of a rigid spacecraft. In [7], adaptive sliding mode fault-tolerant attitude tracking control scheme was developed for flexible spacecraft with partial loss of actuator effectiveness faults, where a neural network was employed to account for system uncertainties and an on-line updating law was used to estimate the upper bound of actuator fault. With the use of fast terminal sliding mode technique, not only fault-tolerant capability but also finite-time convergence were achieved by using an adaptive robust fault-tolerant controller for spacecraft attitude control system in the presence of an uncertain inertia matrix, external disturbances, and two types of actuator faults [8].

On the other hand, the active fault-tolerant attitude control approach reacts to the actuator faults by reconfiguring the controller based on a fault detection and diagnosis (FDD) scheme which provides real-time information about faults, so that the desired attitude maneuver is maintained in spite of actuator faults. Because the attitude kinematics and dynamics of a spacecraft are nonlinear and strongly coupled, only very few research papers consider the active fault-tolerant controller design for spacecraft attitude control system. In [9], actuator failure detection, identification and adaptive reconfigurable controller for spacecraft were proposed, where fast and accurate detection and diagnosis of actuator failure, and convergence of tracking errors to zero can be achieved despite the constraint of control input saturation. In [10], an iterative learning observer was designed to estimate time-varying actuator faults. Based on the FDD scheme developed in [10], an FTC law was reconfigured in [11] to accomplish attitude stabilization maneuver under partial loss of actuator effectiveness faults and external disturbances.

Modern spacecraft often uses redundant actuators to increase the reliability, maneuverability and survivability. This makes the spacecraft attitude control system an over-actuated system [12], [13], which has more control effects than three conventional control effectors. Due to this redundancy, control allocation (CA) is utilized to distribute the desired total control demand over the individual actuators, especially in the case of actuator faults and failures [14], [15]. The benefit of using CA as a means for FTC is that it automatically redistributes control signals to the remaining actuators without reconfiguring the controller [16]. In this paper, we present an effective control allocation scheme for FTC of spacecraft attitude tracking when the actuator fault information estimated by FDD is not precise. By introducing a performance/robustness trade-off factor, a novel performance/robustness trade-off control allocation (PRTCA)

The authors are with EXQUISITUS, Centre for E-City, School of Electrical and Electronic Engineering, Nanyang Technological University, 639798, Singapore {qshen1, edwwang, sqzhu, eekpoh}@ntu.edu.sg

method is proposed to distribute the total desired control command under actuator faults without reconfiguring the controller, and meanwhile to achieve good trade-off between the regular performance given by conventional regularized control allocation (RegCA) with perfect FDD and the robustness given by robust control allocation (RobCA) with imperfect FDD. When different levels of imperfection in FDD are considered, the PRTCA with different level of robustness is carried out, which not only reduces the conservativeness of the RobCA but also ensures the desired regular performance of the RegCA.

II. System Description and Problem Statement

A. Spacecraft Attitude Dynamics

The kinematics and dynamics for the attitude motion of a rigid spacecraft can be expressed by the following equations [17]:

$$\begin{cases} \boldsymbol{J}\dot{\boldsymbol{\omega}} = -\boldsymbol{\omega}^{\times}\boldsymbol{J}\boldsymbol{\omega} + \boldsymbol{D}\boldsymbol{u} + \boldsymbol{d} \\ \dot{\boldsymbol{q}} = \frac{1}{2}(\boldsymbol{q}^{\times} + q_0\boldsymbol{I}_3)\boldsymbol{\omega} \\ \dot{q}_0 = -\frac{1}{2}\boldsymbol{q}^T\boldsymbol{\omega} \end{cases} \tag{1}$$

where $\boldsymbol{J} = \boldsymbol{J}^T \in \mathbb{R}^{3\times 3}$ denotes the positive definite inertia matrix of the spacecraft, $\boldsymbol{\omega} \in \mathbb{R}^3$ is the inertial angular velocity vector of the spacecraft with respect to an inertial frame $\mathcal{I}$ and expressed in the body frame $\mathcal{B}$, $\boldsymbol{Q} = [q_1, q_2, q_3, q_0]^T = [\boldsymbol{q}^T, q_0]^T \in \mathbb{R}^3 \times \mathbb{R}$ denotes the unit quaternion describing the attitude orientation of the body frame $\mathcal{B}$ with respect to inertial frame $\mathcal{I}$ and satisfies the constraint $\boldsymbol{q}^T\boldsymbol{q} + q_0^2 = 1$, $\boldsymbol{I}_3 \in \mathbb{R}^{3\times 3}$ denotes a 3-by-3 identity matrix, $\boldsymbol{u} \in \mathbb{R}^n$ $(n > 3)$ and $\boldsymbol{d} \in \mathbb{R}^3$ denote the control torques produced by the n actuators and the external disturbances, respectively, and $\boldsymbol{D} \in \mathbb{R}^{3\times n}$ is the actuator distribution matrix. The notation $\boldsymbol{x}^{\times} \in \mathbb{R}^{3\times 3}$ for a vector $\boldsymbol{x} = [x_1, x_2, x_3]^T$ is used to represent the skew-symmetric matrix

$$\boldsymbol{x}^{\times} = \begin{bmatrix} 0 & -x_3 & x_2 \\ x_3 & 0 & -x_1 \\ -x_2 & x_1 & 0 \end{bmatrix}. \tag{2}$$

In the case of fault-free, the actual output torques $\boldsymbol{u}$ of n actuators are equal to the desired values $\boldsymbol{u}$ commanded by the controller, i.e., $\boldsymbol{u} = \boldsymbol{u}_c$. When actuator faults are considered, the mathematical fault model of n actuators is described as follows:

$$\boldsymbol{u} = \boldsymbol{E}\boldsymbol{u}_c + \bar{\boldsymbol{u}}, \tag{3}$$

where $\boldsymbol{u}_c = [u_{c1}, u_{c2}, \ldots, u_{cn}]^T \in \mathbb{R}^n$ denotes the command control torque, $\boldsymbol{E} = diag\{e_1, e_2, \ldots, e_n\} \in \mathbb{R}^{n\times n}$ denotes the effectiveness factor matrix of spacecraft actuators with $0 < e_i \leq 1 (i = 1, 2, \ldots, n)$. Note that the case $e_i = 1$ indicates that the ith actuator works normally, and $0 < e_i < 1$ implies that the ith actuator partially loses its effectiveness, but still not totally fail. The vector $\bar{\boldsymbol{u}} = [\bar{u}_1, \bar{u}_2, \ldots, \bar{u}_n]^T \in \mathbb{R}^n$ represents the bounded time-varying additive actuator fault. Hence, the nonlinear attitude dynamics model incorporating actuator faults defined in (3) can be rewritten as the following form:

$$\boldsymbol{J}\dot{\boldsymbol{\omega}} = -\boldsymbol{\omega}^{\times}\boldsymbol{J}\boldsymbol{\omega} + \boldsymbol{D}\left(\boldsymbol{E}\boldsymbol{u}_c + \bar{\boldsymbol{u}}\right) + \boldsymbol{d}. \tag{4}$$

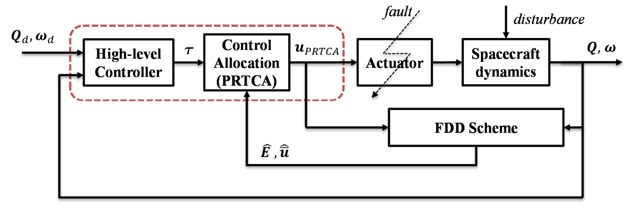

Fig. 1. Structure of the overall spacecraft attitude-tracking scheme.

B. Attitude Error Dynamics

To address the attitude tracking issue, the desired attitude and angular velocity of the spacecraft in the body frame $\mathcal{B}$ with respect to inertial frame $\mathcal{I}$ are denoted by unit quaternion $\boldsymbol{Q}_d = [\boldsymbol{q}_d^T, q_{d0}]^T$ and $\boldsymbol{\omega}_d$, respectively. The attitude tracking error $\boldsymbol{Q}_e = [\boldsymbol{q}_e^T, q_{e0}]^T$ is defined as the relative orientation between the attitude $\boldsymbol{Q}$ and the target attitude $\boldsymbol{Q}_d$, which is computed as

$$\boldsymbol{Q}_e = \boldsymbol{Q}_d^{-1} \otimes \boldsymbol{Q}, \tag{5}$$

where $\boldsymbol{Q}_d^{-1}$ is the inverse or conjugate of the desired quaternion and is determined by $\boldsymbol{Q}_d^{-1} = [-\boldsymbol{q}_d^T, q_{d0}]^T$, and $\otimes$ denotes the quaternion multiplication operator of two unit quaternion $\boldsymbol{Q}_i = [\boldsymbol{q}_i^T, q_{i0}]^T$ and $\boldsymbol{Q}_j = [\boldsymbol{q}_j^T, q_{j0}]^T$, which is defined as follows:

$$\boldsymbol{Q}_i \otimes \boldsymbol{Q}_j = \begin{bmatrix} q_{i0}\boldsymbol{q}_j + q_{j0}\boldsymbol{q}_i + \boldsymbol{q}_i^{\times}\boldsymbol{q}_j \\ q_{i0}q_{j0} - \boldsymbol{q}_i^T\boldsymbol{q}_j \end{bmatrix}. \tag{6}$$

The angular velocity error $\boldsymbol{\omega}_e \in \mathbb{R}^3$ is given by $\boldsymbol{\omega}_e = \boldsymbol{\omega} - \boldsymbol{C}\boldsymbol{\omega}_d$, where $\boldsymbol{C}$ is the rotation matrix, which is defined as

$$\boldsymbol{C} = (q_{e0}^2 - \boldsymbol{q}_e^T\boldsymbol{q}_e)^T\boldsymbol{I_3} + 2\boldsymbol{q}_e\boldsymbol{q}_e^T - 2q_{e0}\boldsymbol{q}_e^{\times}. \tag{7}$$

Consequently, based on the attitude dynamics in (4) with actuator faults, the attitude tracking error system can be described as

$$\begin{cases} \boldsymbol{J}\dot{\boldsymbol{\omega}} = -(\boldsymbol{\omega}_e + \boldsymbol{C}\boldsymbol{\omega}_d)^{\times}\boldsymbol{J}(\boldsymbol{\omega}_e + \boldsymbol{C}\boldsymbol{\omega}_d) \\ \qquad +\boldsymbol{J}(\boldsymbol{\omega}_e^{\times}\boldsymbol{C}\boldsymbol{\omega}_d - \boldsymbol{C}\dot{\boldsymbol{\omega}}_d) + \boldsymbol{D}\left(\boldsymbol{E}\boldsymbol{u}_c + \bar{\boldsymbol{u}}\right) + \boldsymbol{d} \\ \dot{\boldsymbol{q}}_e = \frac{1}{2}(\boldsymbol{q}_e^{\times} + q_{e0}\boldsymbol{I}_3)\boldsymbol{\omega}_e \\ \dot{q}_{e0} = -\frac{1}{2}\boldsymbol{q}_e^T\boldsymbol{\omega}_e \end{cases}. \tag{8}$$

C. Problem Statement

For the over-actuated systems, it is possible to divide the controller design into two steps [13], [18]. In the first step, a high level controller is designed as virtual controller to specify the total desired control efforts to the system. Then, a control allocation algorithm is developed to map the virtual control efforts into individual actuators such that the total actual control signals generated by all actuators amount to the commanded virtual input. Based on such a design philosophy, the overall structure of the proposed fault-tolerant attitude tracking scheme is shown in Fig. 1.

For the high level controller design of attitude tracking system in the first step, define the virtual control torque $\boldsymbol{\tau} \in \mathbb{R}^3$ as

$$\boldsymbol{\tau} = \boldsymbol{D}\boldsymbol{u} = \boldsymbol{D}(\boldsymbol{E}\boldsymbol{u}_c + \bar{\boldsymbol{u}}). \tag{9}$$

Then, the attitude tracking error dynamics with actuator faults in (8) can be rewritten as the following virtual equivalent system

$$\begin{cases} \boldsymbol{J}\dot{\boldsymbol{\omega}} = -(\boldsymbol{\omega}_e + \boldsymbol{C}\boldsymbol{\omega}_d)^{\times}\boldsymbol{J}(\boldsymbol{\omega}_e + \boldsymbol{C}\boldsymbol{\omega}_d) \\ \qquad\quad +\boldsymbol{J}(\boldsymbol{\omega}_e^{\times}\boldsymbol{C}\boldsymbol{\omega}_d - \boldsymbol{C}\dot{\boldsymbol{\omega}}_d) + \boldsymbol{\tau} + \boldsymbol{d} \\ \dot{\boldsymbol{q}}_e = \frac{1}{2}(\boldsymbol{q}_e^{\times} + q_{e0}\boldsymbol{I}_3)\boldsymbol{\omega}_e \\ \dot{q}_{e0} = -\frac{1}{2}\boldsymbol{q}_e^T\boldsymbol{\omega}_e \end{cases}. \tag{10}$$

Since this paper focuses on control allocation design, we assume that there exists the virtual attitude control torques $\boldsymbol{\tau}$ in (10) such that the desired attitude can be obtained and simultaneously external disturbances are suppressed.

In the second step, the estimated fault information will be used in the control allocation design. Here, we also assume that the actuator fault information, $\hat{\boldsymbol{E}} = diag\{\hat{e}_1, \hat{e}_2, \ldots, \hat{e}_n\}$ and $\hat{\bar{\boldsymbol{u}}} = [\hat{\bar{u}}_1, \hat{\bar{u}}_2, \ldots, \hat{\bar{u}}_n]$, could be detected and estimated by an FDD scheme. If the fault information can be identified precisely by the FDD scheme, based on (9), the command control efforts $\boldsymbol{u}_c$ can be computed by solving the following regularized control allocation (RegCA) problem [19]

$$\begin{aligned} \boldsymbol{u}_{RegCA} = \arg \min_{\boldsymbol{u_c}} \Big\{ &\|\hat{\boldsymbol{E}}\boldsymbol{u}_c + \hat{\bar{\boldsymbol{u}}}\|_{\boldsymbol{Q}}^2 \\ &+ h\|\boldsymbol{D}\hat{\boldsymbol{E}}\boldsymbol{u}_c + \boldsymbol{D}\hat{\bar{\boldsymbol{u}}} - \boldsymbol{\tau}\|^2 \Big\}, \end{aligned} \tag{11}$$

where $\boldsymbol{Q}$ is a positive definite weighting matrix and $h > 0$ is a weighting factor.

Because multiple simultaneous faults are considered, decentralized FDD approach [20], hybrid bond graph technique [21], [22], etc, can be used for FDD. However, the estimated fault information $\hat{\boldsymbol{E}}(t)$ and $\hat{\bar{\boldsymbol{u}}}$ may not be precise. Similar to [16], the level of imperfection of fault estimation is introduced, and the relations between the actual fault information and their estimated values are assumed to satisfy

$$\boldsymbol{E} = (\boldsymbol{I}_n - \boldsymbol{\Delta_E})\hat{\boldsymbol{E}}, \qquad \bar{\boldsymbol{u}} = (\boldsymbol{I}_n - \boldsymbol{\Delta}_{\bar{\boldsymbol{u}}})\hat{\bar{\boldsymbol{u}}}, \tag{12}$$

where $\boldsymbol{\Delta_E} = diag\{\delta_{e1}, \delta_{e2}, \ldots, \delta_{en}\}$ and $\boldsymbol{\Delta}_{\bar{\boldsymbol{u}}} = diag\{\delta_{\bar{u}1}, \delta_{\bar{u}2}, \ldots, \delta_{\bar{u}n}\}$, which represent the level of imperfection in the estimations of actuator effectiveness and additive fault, respectively. Thus, during the control allocation, the command control efforts $\boldsymbol{u}_c$ need to be found such that

$$\boldsymbol{\tau} = \boldsymbol{D}[(\boldsymbol{I}_n - \boldsymbol{\Delta_E})\hat{\boldsymbol{E}}\boldsymbol{u}_c + (\boldsymbol{I}_n - \boldsymbol{\Delta}_{\bar{\boldsymbol{u}}})\hat{\bar{\boldsymbol{u}}}]. \tag{13}$$

In light of (13), a robust control allocation (RobCA) is proposed to distribute the virtual control signals to each actuator when the fault information obtained by FDD is not precise, which is expressed as

$$\begin{aligned} \boldsymbol{u}_{RobCA} = \arg \min_{\boldsymbol{u_c}} \max_{\substack{\|\boldsymbol{\Delta_E}\| \le \rho_1, \\ \|\boldsymbol{\Delta}_{\bar{\boldsymbol{u}}}\| \le \rho_2}} \Big\{ &\|\hat{\boldsymbol{E}}\boldsymbol{u}_c + \hat{\bar{\boldsymbol{u}}}\|_{\boldsymbol{Q}}^2 \\ + h\|\boldsymbol{D}(\boldsymbol{I}_n - \boldsymbol{\Delta_E})\hat{\boldsymbol{E}}\boldsymbol{u}_c &+ \boldsymbol{D}(\boldsymbol{I}_n - \boldsymbol{\Delta}_{\bar{\boldsymbol{u}}})\hat{\bar{\boldsymbol{u}}} - \boldsymbol{\tau}\|^2 \Big\}, \end{aligned} \tag{14}$$

where the level of imperfection in fault estimations of the actuator effectiveness $\hat{\boldsymbol{E}}$ and the additive bias fault $\boldsymbol{\Delta}_{\bar{\boldsymbol{u}}}$ are supposed to satisfy $\|\boldsymbol{\Delta_E}\| \le \rho_1$ and $\|\boldsymbol{\Delta}_{\bar{\boldsymbol{u}}}\| \le \rho_2$, respectively. That is, both $\hat{\boldsymbol{E}}$ and $\boldsymbol{\Delta}_{\bar{\boldsymbol{u}}}$ are upper bounded by positive scalars. For the RobCA in (14), the primary objective is to find the optimal $\boldsymbol{u}_c$ by minimizing the the worse-case residual. This achieves some robustness given by the worst residual to control allocation with respect to the imprecision in the fault estimations of the FDD scheme. Since there is no guarantee that $\boldsymbol{\tau}$ is attainable or that the solution of $\boldsymbol{u}_c$ is unique, the secondary objective of the RobCA, which minimizes the power consumption, is also introduced in (14).

III. Control Allocation Design

When the imperfection of fault estimation is large, the RobCA method can achieve better performance than that of the RegCA method because of its strong robustness to estimation uncertainties. However, under small imperfection of fault estimation, the RegCA performs better, and the RobCA method may result in over-conservativeness comparing to the RegCA method as well as a slower transient response. Based on above considerations, a new control allocation scheme is proposed to achieve trade-off between the regular performance given by the RegCA method and the robustness given by the RobCA method. By introducing a performance/robustness trade-off factor, the performance/robustness trade-off control allocation (PRTCA) scheme is designed as follows:

$$\boldsymbol{u}_{PRTCA} = (1-\alpha)\cdot \boldsymbol{u}_{RegCA} + \alpha \cdot \boldsymbol{u}_{RobCA}, \tag{15}$$

where $\alpha \in (0, 1)$ is a positive scalar representing the aforementioned performance/robustness trade-off factor. If the FDD scheme is almost precise (small imperfection of fault estimation), the imperfection factor α should be set to a small value near zero, and the proposed PRTCA achieves a similar regular performance of the RegCA scheme and does not suffer from conservativeness. Otherwise, if the imperfection of fault estimation is large, α should be set to a value near one such that the robustness could be obtained.

Substituting the RegCA from (11) and the RobCA from (14) into the PRTCA defined in (15), the proposed PRTCA scheme is further stated as

$$\begin{aligned} \boldsymbol{u}_{PRTCA} = \arg \min_{\boldsymbol{u}_c} \Big\{ &\|\hat{\boldsymbol{E}}\boldsymbol{u}_c + \hat{\bar{\boldsymbol{u}}}\|_{\boldsymbol{Q}}^2 \\ &+ (1-\alpha)h\|\boldsymbol{D}\hat{\boldsymbol{E}}\boldsymbol{u}_c + \boldsymbol{D}\hat{\bar{\boldsymbol{u}}} - \boldsymbol{\tau}\|^2 \\ &+ \alpha h \max_{\substack{\|\boldsymbol{\Delta_E}\| \le \rho_1, \\ \|\boldsymbol{\Delta}_{\bar{\boldsymbol{u}}}\| \le \rho_2}} \|\boldsymbol{D}(\boldsymbol{I}_n - \boldsymbol{\Delta_E})\hat{\boldsymbol{E}}\boldsymbol{u}_c \\ &+ \boldsymbol{D}(\boldsymbol{I}_n - \Delta_{\bar{u}})\hat{\bar{\boldsymbol{u}}} - \boldsymbol{\tau}\|^2 \Big\}. \end{aligned} \tag{16}$$

To reduce the notational burden, denoting $\boldsymbol{A} = \boldsymbol{D}\hat{\boldsymbol{E}}$, $\boldsymbol{b} = \boldsymbol{\tau} - \boldsymbol{D}\hat{\bar{\boldsymbol{u}}}$, $\boldsymbol{\Delta A} = -\boldsymbol{D}\boldsymbol{\Delta_E}\hat{\boldsymbol{E}}$, and $\boldsymbol{\Delta b} = \boldsymbol{D}\boldsymbol{\Delta}_{\bar{\boldsymbol{u}}}\hat{\bar{\boldsymbol{u}}}$. Because $\|\boldsymbol{\Delta_E}\| \le \rho_1$, $\|\boldsymbol{\Delta}_{\bar{\boldsymbol{u}}}\| \le \rho_2$, we can get that $\|\boldsymbol{\Delta A}\| \le \rho_A$, $\|\boldsymbol{\Delta b}\| \le \rho_b$, where $\rho_A = \rho_1\|\boldsymbol{D}\|\|\hat{\boldsymbol{E}}\|$, $\rho_b = \rho_2\|\boldsymbol{D}\|\|\hat{\bar{\boldsymbol{u}}}\|$. As a consequence, the proposed PRTCA becomes

$$\boldsymbol{u}_{PRTCA} = \arg \min_{\boldsymbol{u_c}} \Big\{ \|\hat{\boldsymbol{E}}\boldsymbol{u}_c + \hat{\hat{\boldsymbol{u}}}\|^2_{\boldsymbol{Q}} + (1-\alpha)h\|\boldsymbol{A}\boldsymbol{u}_c - \boldsymbol{b}\|^2 + \alpha h \max_{\substack{\|\boldsymbol{\Delta A}\|\le\rho_A,\\ \|\boldsymbol{\Delta b}\|\le\rho_b}} \|(\boldsymbol{A}+\boldsymbol{\Delta A})\boldsymbol{u}_c - (\boldsymbol{b}+\boldsymbol{\Delta b})\|^2 \Big\}. \quad (17)$$

It is verified that this problem is equivalent to a problem of the form [23]

$$\boldsymbol{u}_{PRTCA} = \arg \min_{\boldsymbol{u_c}} \Big\{ \|\hat{\boldsymbol{E}}\boldsymbol{u}_c + \hat{\hat{\boldsymbol{u}}}\|^2_{\boldsymbol{Q}} + (1-\alpha)h\|\boldsymbol{A}\boldsymbol{u}_c - \boldsymbol{b}\|^2 + \alpha h \max_{\|\boldsymbol{z}\|\le\phi(\boldsymbol{u_c})} ||\boldsymbol{A}\boldsymbol{u}_c - \boldsymbol{b} + \boldsymbol{z}||^2 \Big\}, \quad (18)$$

where $\phi(\boldsymbol{u}_c)$ is a function defined as $\phi(\boldsymbol{u}_c) = \rho_A||\boldsymbol{u}_c|| + \rho_b$.

In order to get the solution of the above PRTCA, the inner maximization problem is solved first, then followed by the outer minimization problem [24]. For the inner maximization problem, the maximum

$$C(\boldsymbol{u}_c) \triangleq \max_{||\boldsymbol{z}||\le\phi(\boldsymbol{u}_c)} \alpha h||\boldsymbol{A}\boldsymbol{u}_c - \boldsymbol{b} + \boldsymbol{z}||^2 \quad (19)$$

is a convex function in $\boldsymbol{u}_c$. In addition, it is noted that the inequality constraint is convex in $\boldsymbol{z}$, so that the maximum over $\boldsymbol{z}$ is achieved at the boundary, i.e. $||\boldsymbol{z}|| = \phi(\boldsymbol{u}_c)$. Introducing a Lagrange multiplier λ, the constrained maximization problem in (19) is transformed into the following unconstrained problem

$$\max_{\boldsymbol{z},\lambda} \left[\alpha h||\boldsymbol{A}\boldsymbol{u}_c - \boldsymbol{b} + \boldsymbol{z}||^2 - \lambda(||\boldsymbol{z}||^2 - \phi^2(\boldsymbol{u}_c))\right]. \quad (20)$$

Since the original problem has an inequality constraint, the Lagrange multiplier must be nonnegative, i.e., $\lambda \ge 0$. Differentiating (20) with respect to $\boldsymbol{z}$ and λ, the following expressions can be obtained

$$(\lambda^* - \alpha h)\boldsymbol{z}^* = \alpha h(\boldsymbol{A}\boldsymbol{u}_c - \boldsymbol{b}), \quad ||\boldsymbol{z}^*|| = \phi(\boldsymbol{u}_c), \quad (21)$$

where $\boldsymbol{z}^*$ and λ^* denote the optimal solution of the maximization problem in (20).

Moreover, computing the Hessian of the cost in (20) with respect to $\boldsymbol{z}$, and let it be negative semi-definite when $\lambda = \lambda^*$, it can be found that the optimal solution of λ^* should satisfy $\lambda^* \ge \alpha h$. Thus, in view of (21), the maximum cost in (20) is given by

$$C(\boldsymbol{u}_c) = \frac{\alpha h \lambda^*}{\lambda^* - \alpha h}||\boldsymbol{A}\boldsymbol{u}_c - \boldsymbol{b}||^2 + \lambda^*\phi^2(\boldsymbol{u}_c). \quad (22)$$

Substituting (22) into the original problem, the PRTCA problem is equivalent to the following minimization problem:

$$\begin{aligned}\boldsymbol{u}_{PRTCA} &= \arg \min_{\boldsymbol{u}_c} \Big\{ ||\hat{\boldsymbol{E}}\boldsymbol{u}_c + \hat{\hat{\boldsymbol{u}}}||^2_{\boldsymbol{Q}} + (1-\alpha)h||\boldsymbol{A}\boldsymbol{u}_c - \boldsymbol{b}||^2 + C(\boldsymbol{u}_c) \Big\} \\ &= \arg \min_{\boldsymbol{u}_c} \Big\{ ||\hat{\boldsymbol{E}}\boldsymbol{u}_c + \hat{\hat{\boldsymbol{u}}}||^2_{\boldsymbol{Q}} + \left(h + \frac{\alpha^2 h^2}{\lambda^* - \alpha h}\right) \times ||\boldsymbol{A}\boldsymbol{u}_c - \boldsymbol{b}||^2 + \lambda^*\phi^2(\boldsymbol{u}_c) \Big\}. \quad (23)\end{aligned}$$

Next, we need to solve the outer minimization problem as shown in (23). In order to reduce the computation burden, we will reduce the problem to a one-dimensional search problem. For this purpose, the following function with two independent variables $\boldsymbol{u}_c$ and λ is introduced,

$$R(\boldsymbol{u}_c, \lambda) = \frac{\alpha h \lambda}{\lambda - \alpha h}||\boldsymbol{A}\boldsymbol{u}_c - \boldsymbol{b}||^2 + \lambda\phi^2(\boldsymbol{u}_c), \quad (24)$$

where λ belongs to the interval $[\alpha h, +\infty)$. Then, it is found that the cost of the inner maximization in (19) is equal to the constrained minimization problem over the scalar Lagrange multiplier λ [24],

$$C(\boldsymbol{u}_c) = \arg \min_{\lambda\ge\alpha h} R(\boldsymbol{u}_c, \lambda). \quad (25)$$

As a result, the original problem turns out to be equivalent to

$$\begin{aligned}\boldsymbol{u}_{PRTCA} &= \arg \min_{\boldsymbol{u}_c} \Big\{ ||\hat{\boldsymbol{E}}\boldsymbol{u}_c + \hat{\hat{\boldsymbol{u}}}||^2_{\boldsymbol{Q}} + (1-\alpha)h||\boldsymbol{A}\boldsymbol{u}_c - \boldsymbol{b}||^2 + \min_{\lambda\ge\alpha h} R(\boldsymbol{u}_c, \lambda) \Big\} \\ &= \arg \min_{\lambda\ge\alpha h} \min_{\boldsymbol{u}_c} J(\boldsymbol{u}_c, \lambda) \quad (26)\end{aligned}$$

where $J(\boldsymbol{u}_c, \lambda) = ||\hat{\boldsymbol{E}}\boldsymbol{u}_c + \hat{\hat{\boldsymbol{u}}}||^2_{\boldsymbol{Q}} + W(\lambda)||(\boldsymbol{A}\boldsymbol{u}_c - \boldsymbol{b})||^2 + \lambda\phi^2(\boldsymbol{u}_c)$, and $W(\lambda) = h + \frac{\alpha^2 h^2}{\lambda - \alpha h}$.

Note that, because $J(\boldsymbol{u}_c, \lambda)$ is a quadratic function, it is possible to derive a closed-form expression for the solution of the innermost minimization in (26) with respect to $\boldsymbol{u}_c$ for fixed value of the Lagrange multiplier λ. Since $\phi(\boldsymbol{u}_c) = \rho_A||\boldsymbol{u}_c|| + \rho_b$, taking the derivative of $J(\boldsymbol{u}_c, \lambda)$ with respect to $\boldsymbol{u}_c$, it follows that

$$\left[\boldsymbol{M}(\lambda) + \lambda\rho_A\left(\rho_A + \frac{\rho_b}{||\boldsymbol{u}_c||}\right)\boldsymbol{I}_N\right]\boldsymbol{u}_c(\lambda) = \boldsymbol{N}(\lambda) \quad (27)$$

where $\boldsymbol{M}(\lambda) = \hat{\boldsymbol{E}}^T\boldsymbol{Q}\hat{\boldsymbol{E}} + W(\lambda)\boldsymbol{A}^T\boldsymbol{A}$, and $\boldsymbol{N}(\lambda) = W(\lambda)\boldsymbol{A}^T\boldsymbol{b} - \hat{\boldsymbol{E}}^T\boldsymbol{Q}\hat{\hat{\boldsymbol{u}}}$. Then, for any nonzero $\boldsymbol{u}_c$, we can get

$$\boldsymbol{u}_c(\lambda) = \left[\boldsymbol{M}(\lambda) + \lambda\rho_A\left(\rho_A + \frac{\rho_b}{||\boldsymbol{u}_c||}\right)\boldsymbol{I}_n\right]^{-1}\boldsymbol{N}(\lambda) \quad (28)$$

Because $\boldsymbol{u}_c$ appears on both sides of the equality, $\boldsymbol{u}_c$ can not be obtained directly. With a view to tackle the above challenge, two cases are considered.

Case I: If $\rho_b = 0$, the term $||\boldsymbol{u}_c||$ will disappear on the right-hand side of the expression in (28). In this case, the expression for $\boldsymbol{u}_c(\lambda)$ is given by

$$\boldsymbol{u}_c(\lambda) = \left[\boldsymbol{M}(\lambda) + \lambda\rho_A^2 I\right]^{-1}\boldsymbol{D}(\lambda). \quad (29)$$

Case II: If $\rho_b \ne 0$, $\boldsymbol{u}_c$ is included on both sides of (28). To solve u_c , the scalar $\beta = ||\boldsymbol{u}_c||$ is introduced. As a result, the equation (28) is convert to the following equation with a scalar variable β:

$$\beta^2 - \boldsymbol{N}^T(\lambda)\left[\boldsymbol{M}(\lambda) + \lambda\rho_A\left(\rho_A + \frac{\rho_b}{\beta}\right)\boldsymbol{I}_n\right]^{-2}\boldsymbol{N}(\lambda) = 0. \quad (30)$$

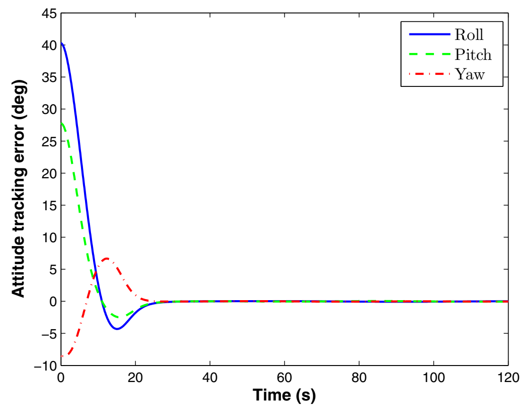

Fig. 2. Attitude tracking error (deg).

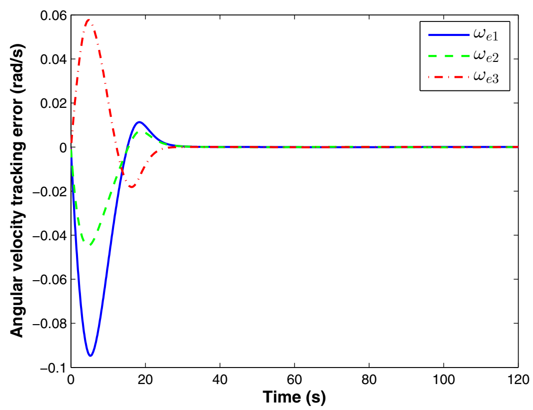

Fig. 3. Angular velocity tracking error (rad/s).

It can be shown that a unique solution $\beta^*(\lambda) > 0$ exists for this equation if $\lambda\rho_A\rho_b \le ||\boldsymbol{N}(\lambda)||$. Otherwise, $\beta^*(\lambda) = 0$.

Now, let $J(\lambda)$ denote the minimum value of $J(\boldsymbol{u}_c, \lambda)$ over $\boldsymbol{u}_c$, i.e.,

$$J(\lambda) = \min_{\boldsymbol{u}_c} J(u_c, \lambda) = J(\boldsymbol{u}_c^*(\lambda), \lambda) \quad (31)$$

$$= ||\hat{\boldsymbol{E}}\boldsymbol{u}_c^*(\lambda) + \hat{\bar{\boldsymbol{u}}}||_{\boldsymbol{Q}}^2 + W(\lambda)||\boldsymbol{A}\boldsymbol{u}_c^*(\lambda) - \boldsymbol{b}||^2 + \lambda\phi^2(\boldsymbol{u}_c^*(\lambda)) \quad (32)$$

Finally, the PRTCA problem can be solved by determining the λ^* from the following scalar-valued optimization problem

$$\lambda^* = arg \min_{\lambda \ge \alpha h} J(\lambda). \quad (33)$$

Because the function $J(\lambda)$ is unimodal, the minimization problem (33) is always well-posed such that an unique minimum on its domain is attainable.

IV. Simulations

To study the effectiveness and performance of the proposed PRTCA-based FTC strategies, numerical simulations have been carried out using the rigid spacecraft system given

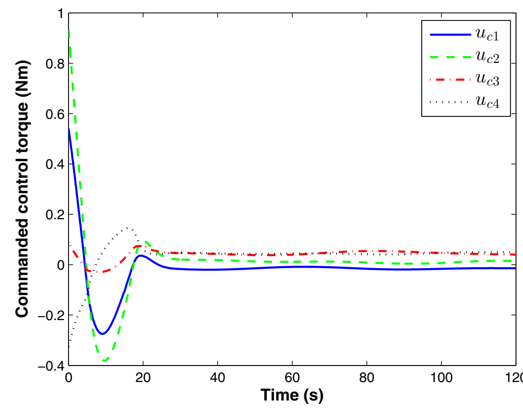

Fig. 4. Commanded torques for attitude tracking (Nm).

in (1) under actuator faults modeled in (3). The spacecraft is assumed to have the inertia matrix of

$$\boldsymbol{J} = \begin{bmatrix} 20 & 0 & 0.9 \\ 0 & 17 & 0 \\ 0.9 & 0 & 15 \end{bmatrix} kg \cdot m^2.$$

The external disturbances are assumed as

$$\boldsymbol{d} = 10^{-3} \times \begin{bmatrix} 3\cos(0.1t) + 4\sin(0.03t) - 1 \\ -1.5\sin(0.02t) - 3\cos(0.05t) + 1.5 \\ 2\sin(0.1t) - 1.5\cos(0.04t) + 1 \end{bmatrix} Nm.$$

In order to achieve three axes control of a spacecraft, at least three actuators are required to force the attitude to follow a commanded attitude trajectory. In fact, four reaction wheels are considered as actuators in the simulation, which indicates the existence of actuator redundancy in the attitude control system. The distribution matrix of four reaction wheels is as follows:

$$\boldsymbol{D} = \frac{1}{\sqrt{3}} \begin{bmatrix} -1 & -1 & 1 & 1 \\ 1 & -1 & -1 & 1 \\ 1 & 1 & 1 & 1 \end{bmatrix}.$$

During the attitude tracking maneuver, both loss of effectiveness faults and additive increased bias faults are considered. The scenarios of partial loss of actuator faults are described as

$$\begin{cases} e_1(t) = 0.5 + 0.08\sin(0.05t) \\ e_2(t) = 0.6 + 0.1\sin(0.02t) \\ e_3(t) = 0.5 + 0.1\sin(0.08t) \\ e_4 = 1, \end{cases}$$

and the increased bias faults are

$$\begin{cases} \bar{u}_1(t) = 0 \\ \bar{u}_2(t) = 0 \\ \bar{u}_3(t) = -0.03 - 0.004\sin(0.02t) \\ \bar{u}_4(t) = -0.04 + 0.005\sin(0.02t). \end{cases}$$

Here we suppose that the maximum imperfection in FDD is 20%, and the estimated fault information by FDD is

$$\begin{cases} \hat{e}_1 = 0.5 \\ \hat{e}_1 = 0.6 \\ \hat{e}_1 = 0.5 \\ \hat{e}_1 = 1 \end{cases}, \quad \begin{cases} \hat{\bar{u}}_1 = 0 \\ \hat{\bar{u}}_2 = 0 \\ \hat{\bar{u}}_3 = -0.03 \\ \hat{\bar{u}}_4 = -0.04 \end{cases}$$

To implement the PRTCA-based FTC scheme, a robust adaptive controller from [6] is used as high-level virtual controller to produce the total control torques as well as reject external disturbances. The initial orientation of the spacecraft is $\boldsymbol{Q}(0) = [0.25,\ 0.2,\ -0.15,\ 0.9354]^T$ with a zero initial body angular velocity. The desired reference angular velocity is given as

$$\boldsymbol{\omega}_d(t) = 0.001 \times \left[\cos(\frac{\pi t}{50}),\ \sin(\frac{\pi t}{30}),\ \cos(\frac{\pi t}{20})\right]^T \text{ rad/s.}$$

For PRTCA, the weighting matrix $\boldsymbol{Q}$ and weighting scalar h in (15) have been chosen as $\boldsymbol{Q} = \boldsymbol{I}_4$ and $h = 1 \times 10^4$, respectively. Since there is 20% imperfection in fault estimation, robustness of control allocation should be reinforced. In view of above consideration, the performance/robustness trade-off factor α is chosen as $\alpha = 0.8$.

The simulation results are shown in Figs. 2-4. Figs. 2-3 depict the responses of the attitude tracking error and angular velocity error under the proposed PRTCA-based FTC strategy, respectively. It can be observed that high tracking precision and good tracking process are obtained even in the presence of external disturbances and actuator faults. The command control torque generated by the PRTCA is shown in Fig. 4. It is clear that the proposed PRTCA automatically redistributes the virtual control torques to four reaction wheels, while maintaining the robustness to imprecise FDD estimation.

V. Conclusions

In this paper, CA-based FTC strategy has been proposed for spacecraft attitude tracking system. By compromising the regular performance provided by the RegCA scheme and the robustness provided by the RobCA scheme, the PRTCA scheme is introduced when there exist imprecision in FDD scheme. The PRTCA problem is formulated as a min-max optimization problem, and it could be solved in a way similar to robust least-squares method. The feasibility and effectiveness of the proposed PRTCA-based FTC scheme is tested in simulation, which shows that actuator faults could be handled without reconfiguring the controller. As one of the future works, actuator saturation and rate constraint should be taken into account during the PRTCA design.

References

[1] M. Blanke, R. Izadi-Zamanabadi, S. A. Bosh, and C. P. Lunau, "Fault-tolerant control systems - a holistic view," *Control Engineering Practice*, vol. 5, no. 5, pp. 693–702, May 1997.

[2] R. J. Patton, "Fault-tolerant control systems: the 1997 situation," in *Proceedings of the IFAC symposium on fault detection supervision and safety for technical processes*, vol. 3, 1997, pp. 1033–1054.

[3] M. Blanke, M. Kinnaert, J. Lunze, and M. Staroswiecki, *Diagnosis and Fault-Tolerant Control*, 2nd ed. Berlin, Germany: Springer, 2006.

[4] Godard, "Fault tolerant control of spacecraft," Ph.D. dissertation, Ryerson University, Toronto, Ontario, Canada, 2010.

[5] Y. M. Zhang and J. Jiang, "Bibliographical review on reconfigurable fault-tolerant control systems," *Annual Reviews in Control*, vol. 32, no. 2, pp. 229–252, Dec. 2008.

[6] W. C. Cai, X. H. Liao, and Y. D. Song, "Indirect robust adaptive fault-tolerant control for attitude tracking of spacecraft," *Journal of Guidance, Control, and Dynamics*, vol. 31, no. 5, pp. 1456–1463, Sep.-Oct. 2008.

[7] B. Xiao, Q. L. Hu, and Y. M. Zhang, "Adaptive sliding mode fault tolerant attitude tracking control for flexible spacecraft under actuator saturation," *IEEE Transactions on Control Systems Technology*, vol. 20, no. 6, pp. 1605–1612, Nov. 2012.

[8] Q. Shen, D. Wang, S. Zhu, E. K. Poh, and T. Liu, "Adaptive robust fault-tolerant attitude control of spacecraft with finite-time convergence," in *Proc. 9th Asian Control Conference*, Istanbul, 2013.

[9] J. D. Boskovic, S.-M. Li, and R. K. Mehra, "Intelligent control of spacecraft in the presence of actuator failures," in *Proc. 38th IEEE Conf. Decision Control*, vol. 5, Phoenix, AZ, 1999, pp. 4472–4477.

[10] W. Chen and M. Saif, "Observer-based fault diagnosis of satellite systems subject to time-varying thruster faults," *Journal of Dynamic Systems, Measurement, and Control*, vol. 129, no. 3, pp. 352–356, 2007.

[11] B. Xiao, Q. Hu, and M. I. Friswell, "Active fault-tolerant attitude control for flexible spacecraft with loss of actuator effectiveness," *International Journal of Adaptive Control and Signal Processing*, vol. 27, no. 11, pp. 925–943, 2013.

[12] M. W. Oppenheimer, D. B. Doman, and M. A. Bolender, "Control allocation for over-actuated systems," in *14th Mediterranean Conference on Control and Automation*, 2006.

[13] T. A. Johansen and T. I. Fossen, "Control allocation-a survey," *Automatica*, vol. 49, no. 5, pp. 1087–1103, May 2013.

[14] J. J. Burken, P. Lu, Z. Wu, and C. Bahm, "Two reconfigurable flight-control design methods: Robust servomechanism and control allocation," *Journal of Guidance, Control, and Dynamics*, vol. 24, no. 3, pp. 482–493, 2001.

[15] A. Casavola and E. Garone, "Fault-tolerant adaptive control allocation schemes for overactuated systems," *International Journal of Robust and Nonlinear Control*, vol. 20, no. 17, pp. 1958–1980, 2010.

[16] H. Alwi and C. Edwards, "Fault tolerant control using sliding modes with on-line control allocation," *Automatica*, vol. 44, no. 7, pp. 1859–1866, Jul. 2008.

[17] M. J. Sidi, *Spacecraft Dynamics and Control*. Cambridge, U.K.: Cambridge, NY: Cambridge University Press, 1997.

[18] O. Harkegard and S. T. Glad, "Resolving actuator redundancy-optimal control vs. control allocation," *Automatica*, vol. 41, no. 1, pp. 137–144, 2005.

[19] J. A. M. Petersen and M. Bodson, "Constrained quadratic programming techniques for control allocation," *IEEE Transactions on Control Systems Technology*, vol. 14, no. 1, pp. 91–98, 2006.

[20] J. D. Boskovic and R. K. Mehra, "A decentralized fault-tolerant control system for accommodation of failures in higher-order flight control actuators," *IEEE Transactions on Control Systems Technology*, vol. 18, no. 5, pp. 1103–1115, Sep. 2010.

[21] M. Yu, D. Wang, and M. Luo, "Model-based prognosis for hybrid systems with mode-dependent degradation behaviors," *IEEE Transactions on Industrial Electronics*, vol. 61, no. 1, pp. 546–554, Jan. 2014.

[22] M. Yu and D. Wang, "Model-based health monitoring for a vehicle steering system with multiple faults of unknown types," *IEEE Transactions on Industrial Electronics*, vol. 61, no. 7, pp. 3574–3586, Jul. 2014.

[23] V. H. Nascimento and A. H. Sayed, "Optimal state regulation for uncertain state-space models," in *Proc. Amer. Control Conf.*, 1999, pp. 419–424.

[24] A. Sayed, V. Nascimento, and F. Cipparrone, "A regularized robust design criterion for uncertain data," *SIAM Journal on Matrix Analysis and Applications*, vol. 23, no. 4, pp. 1120–1142, 2002.